

CALIBRATION OF THE MASS-TEMPERATURE RELATION FOR CLUSTERS OF GALAXIES USING WEAK GRAVITATIONAL LENSING¹

KRISTIAN PEDERSEN

Dark Cosmology Centre, Niels Bohr Institute, University of Copenhagen, Juliane Maries Vej 30, DK-2100, Copenhagen Ø, Denmark

HÅKON DAHLE²

Institute of Theoretical Astrophysics, University of Oslo, P.O. Box 1029, Blindern, N-0315 Oslo, Norway

Submitted to ApJ

ABSTRACT

The main uncertainty in current determinations of the power spectrum normalization, σ_8 , from abundances of X-ray luminous galaxy clusters arises from the calibration of the mass-temperature relation. We use our weak lensing mass determinations of 30 clusters from the hitherto largest sample of clusters with lensing masses, combined with X-ray temperature data from the literature, to calibrate the normalization of this relation at a temperature of 8 keV, $M_{8\text{keV}} = (0.78 \pm 0.14) h^{-1} 10^{15} M_\odot$, at $z \approx 0.23$. This normalization is consistent with previous lensing-based results based on smaller cluster samples, and with some predictions from numerical simulations, but higher than most normalizations based on X-ray derived cluster masses. Assuming the theoretically expected slope $\alpha = 3/2$ of the mass-temperature relation, we derive $\sigma_8 = 0.88 \pm 0.09$ for a spatially-flat Λ CDM universe with $\Omega_m = 0.3$. There is significant intrinsic scatter in the mass-temperature relation indicating that this relation may not be very tight, at least at the high mass end. Furthermore, we find that for a given mass dynamically non-relaxed clusters are $75 \pm 40\%$ hotter than relaxed clusters.

Subject headings: Cosmology: observations — cosmological parameters — dark matter — gravitational lensing — Galaxies: clusters

1. INTRODUCTION

The abundance of massive clusters of galaxies provides sensitive constraints on the cosmological parameters that govern structure growth in the universe. However, these studies require reliable mass measurements for large samples of clusters with well-understood selection criteria. Cluster mass measurements used for such studies have traditionally come from virial analysis of the velocity dispersion measurements of cluster galaxies (e.g., Frenk et al. 1990; Carlberg et al. 1997; Borgani et al. 1999), or X-ray temperature measurements of the hot intra-cluster gas under the assumption that the gas is in hydrostatic equilibrium (for a review see Rosati, Borgani & Norman 2002). Satellite observatories such as ROSAT, ASCA, XMM-Newton and *Chandra* have made increasingly accurate X-ray temperature measurements of clusters, and have produced well-defined cluster samples of sufficient size to accurately measure the X-ray temperature and luminosity functions (e.g. Henry 2004; Böhringer et al. 2002). However, the relation between cluster mass and X-ray temperature and luminosity, respectively, must be determined to convert these into a reliable cluster mass function.

X-ray luminosities are available for large samples of clusters, but the X-ray luminosity is highly sensitive to the complex physics of cluster cores, making it challenging to relate to cluster mass. Measuring X-ray temperatures is observationally much more demanding, but the X-ray temperature is mainly determined by gravitational processes and is hence more directly related to cluster mass than X-ray luminosity. Both from simulations and observations the intrinsic scatter

in mass around the mass-temperature relation is thus found to be much smaller ($\Delta M/M \approx 0.15$, Evrard, Metzler, & Navarro 1996; Borgani et al. 2004; Sanderson et al. 2003; Vikhlinin et al. 2005) than the scatter in mass around the mass-luminosity relation ($\Delta M/M \approx 0.4$, Reiprich & Böhringer 2002).

Two different routes have been followed for determining the mass-temperature relation. Most studies have used a small sample (up to about a dozen) of supposedly well understood clusters for which the assumptions underlying the mass determination should be fulfilled to a high degree. The main concern for this approach is that the selected clusters may not be representative of the whole cluster population, and therefore the derived mass-temperature relation may only apply to a subset of clusters. Alternatively, the mass-temperature relation may be determined from a large sample of more objectively selected clusters. This is more fruitful when comparing such a locally determined mass-temperature relation to a sample of high-redshift clusters where the data quality does not allow a similar selection of the “most suitable” clusters. Also, mass-temperature relations derived from simulations are usually based on a large range of simulated clusters with no pre-selection. Hence it is most appropriate to compare observationally obtained mass-temperature relations determined from all available clusters to the relations from simulations. On the other hand, for some of the clusters in such a sample the hydrostatic assumption may be invalid, making X-ray based mass determinations unreliable for a subset of the clusters. A larger scatter (which may not be symmetric) around the mean mass-temperature relation may be expected, when such clusters are included.

There are still poorly understood systematic uncertainties associated with establishing the mass-temperature relation. The normalization of the mass-temperature relation based on cluster masses determined from X-ray data (Finoguenov, Reiprich, & Böhringer 2001; Vikhlinin et al. 2005; Arnaud, Pointecouteau, & Pratt 2005), tend to differ significantly be-

Electronic address: hdahle@astro.uio.no

¹ Based on observations made with the Nordic Optical Telescope, operated on the island of La Palma jointly by Denmark, Finland, Iceland, Norway, and Sweden, in the Spanish Observatorio del Roque de los Muchachos of the Instituto de Astrofísica de Canarias

² Visiting observer, University of Hawaii 2.24m Telescope at Mauna Kea Observatory, Institute for Astronomy, University of Hawaii

tween studies, and from the expectations based on numerical simulations (e.g., Evrard et al. 1996; Eke et al. 1998; Pen 1998; Borgani et al. 2004). The determination of this normalization, T_\star (see eq. 3), is currently the dominating source of discrepancies between the reported values for the power spectrum normalization on the scale of galaxy clusters, σ_8 , derived from the observed cluster temperature function (Huterer & White 2002; Seljak 2002; Pierpaoli et al. 2003; Henry 2004). Observations using X-ray based mass determinations have traditionally favored high values of T_\star (and hence low values of σ_8), while simulations have favored somewhat lower values of T_\star .

Gravitational lensing provides an opportunity to measure cluster masses without invoking the assumption of hydrostatic equilibrium in the hot intra-cluster gas implicit in the X-ray based mass determinations. Also, in this case the measurement of cluster mass is truly independent of the X-ray temperature measurement. Hjorth, Oukbir & van Kampen (1998) used weak gravitational mass measurements for eight clusters drawn from the literature to find a relation between mass over cluster-centric radius and temperature. They determined a normalization of this relation consistent with the value predicted by Evrard et al. (1996), but with a preference for somewhat higher cluster masses, if the redshift scaling of equation 3 is assumed. However, Smith et al. (2005; hereafter S05) determined a mass-temperature relation with a normalization significantly lower than indicated by the Hjorth et al. (1998) study. S05 based their results on a sample of 10 clusters with weak lensing masses and temperatures determined from *Chandra* data.

Here, we present a new weak gravitational lensing-based measurement of the normalization of the mass-temperature relation. The main improvements with respect to the work of Hjorth et al. (1998) and S05 is that we use a significantly larger cluster sample which represents a significant fraction of all the clusters in an even larger sample with well-defined objective selection criteria (Dahle et al. 2002; H. Dahle 2006, in preparation). An additional improvement over the work of Hjorth et al. (1998) is that the weak lensing analysis has been performed in a consistent way for all clusters, using the same shear estimator and making the same assumptions about e.g., the typical redshift of the lensed galaxy population and the degree of contamination by cluster galaxies. We note that the early data set of clusters with published weak lensing masses used by Hjorth et al. (1998) is biased at some level towards systems that were observed because of “extreme” properties, such as being the hottest or most X-ray luminous system known at the time, or having a large number of strongly gravitationally lensed arcs. Furthermore, we note that our gravitational lensing measurements are made at larger radii than probed by S05, requiring smaller extrapolations to estimate the mass within e.g., the virial radii of the clusters.

The data set used for the analysis is described in § 2, our results for the mass-temperature relation and σ_8 are presented in § 3, and our results are compared to other work and the implications discussed in § 4.

Except when specifically noted otherwise (for easy comparison to previous results using different cosmologies), we assume a spatially-flat cosmology with a cosmological constant ($\Omega_m = 0.3$, $\Omega_\Lambda = 0.7$), and the Hubble parameter is given by $H_0 = 100h \text{ km s}^{-1} \text{Mpc}^{-1}$.

2. DATA SET

2.1. Weak lensing data

Our weak lensing data set is a sample of 30 clusters, of which 28 were included in the weak lensing cluster sample of Dahle et al. (2002). Data for two additional clusters come from a recent extension of this data set (H. Dahle 2006, in preparation). The clusters targeted for these weak lensing studies were generally selected to lie above an X-ray luminosity limit $L_{X,0.1-2.4\text{keV}} \geq 1.2 \times 10^{45} \text{ ergs s}^{-1}$ (this luminosity limit is for our chosen cosmology with $h = 0.5$) and within a redshift range $0.15 < z_{\text{cl}} < 0.35$. The observed clusters were selected from the X-ray luminous cluster samples of Briel & Henry (1993) and Ebeling et al. (1996; 1998; 2000). The observations were made with the 8192^2 UH8K mosaic CCD camera and the 2048^2 Tek CCD camera at the 2.24m University of Hawaii Telescope and with the 2048^2 ALFOSC CCD camera at the 2.56m Nordic Optical Telescope. The observations and data reduction of the data set used for the weak lensing mass measurements are described in detail by Dahle et al. (2002).

Major efforts are being made to improve the methods for the estimation of weak gravitational lensing, particularly in connection with ongoing and future studies of “cosmic shear” based on wide-field optical surveys. The requirements for the precision of shear estimates in these surveys are substantially more stringent than for weak lensing observations of massive clusters, given the significantly weaker lensing effects measured in random fields.

In this work, we have used the shear estimator of Kaiser (2000), which was “blind-tested” (along with several other shear estimators) by Heymans et al. (2005), using simulated lensing data. The shear estimator of Kaiser (2000) is more mathematically rigorous than the currently most widely used shear estimator (Kaiser, Squires, & Broadhurst 1995), but it displays a significant non-linear response to shear, unlike most other shear estimators. If we correct our shear values using a quadratic term based on the test results of Heymans et al. (2005), we find that most cluster masses stay within $\pm 15\%$ of the mass calculated based on uncorrected shear values. Furthermore, the change in average cluster mass is $< 2\%$, i.e., there is very little systematic shift in mass. In the end, we chose not to apply this correction, since it would, in a few cases, require extrapolations outside the range of shear values over which the shear estimator has been tested. For more details about the practical implementation of this shear estimator, see Dahle et al. (2002).

To convert the measurements of weak gravitational shear into actual cluster masses, the distances to the background galaxies need to be known. The background galaxy redshifts were estimated from spectroscopic and photometric redshifts in the Hubble Deep Field (for details, see Dahle et al. 2002). For our data set and chosen cosmological model, the average value of the ratio between the lens-source and observer-source angular diameter distances, $\beta \equiv D_{ls}/D_s$, is well approximated by the relation $\langle \beta \rangle = 1.37z_{\text{cl}}^2 - 2.00z_{\text{cl}} + 1.01$ within the redshift range of our cluster sample.

The observable galaxy shape distortions caused by gravitational lensing provide a measurement of the reduced tangential shear, $g_T = \gamma_T/(1 - \kappa)$, where γ_T is the tangential component of the shear and κ is the convergence. We fit an NFW-type mass density profile,

$$\rho(r) = \frac{\delta_c \rho_c(z)}{(r/r_s)(1+r/r_s)^2} \quad (1)$$

(Navarro, Frenk, & White 1997), to the observed reduced shear profile $g_T(r)$ of each cluster. Here, $\rho_c(z)$ is the critical density of the universe at the redshift of the cluster, and

$$\delta_c = \frac{200}{3} \frac{c_{200}^3}{\ln(1+c_{200}) - c_{200}/(1+c_{200})}. \quad (2)$$

We assumed a concentration parameter $c_{200} = c_{\text{vir}}/1.194 = 4.9/(1+z)$, corresponding to the median halo concentration predicted by Bullock et al. (2001) for a $M_{\text{vir}} \simeq 8 \times 10^{14} M_\odot$ cluster from simulations of dark matter halos in a Λ CDM universe. Here, $c_{200} = r_{200c}/r_s$, and $c_{\text{vir}} = r_{\text{vir}}/r_s$, where r_{200c} is defined as the radius within which the average mass density is 200 times the critical density $\rho_c(z)$, and r_{vir} is the virial radius of the cluster.

The lensing properties of the NFW model have been calculated by Bartelmann (1996) and Wright & Brainerd (2000). From our fit, we calculated M_{500c} , the mass enclosed by the radius r_{500c} . The mass estimates are listed in Table 1. The shear measurements used for the fit were made at clustercentric radii $50'' < r < 180''$ for the clusters that were observed with 2048^2 CCD cameras and $150'' < r < 550''$ for the clusters that were observed with the UH8K camera. By comparison, we find r_{500c} values typically in the range $300'' < r_{500c} < 600''$ for the clusters we study here. Since we extrapolate an NFW profile, assuming the median concentration parameter given above, any intrinsic scatter in c_{vir} will introduce an extra uncertainty in the cluster mass estimates. However, we find that the level of scatter predicted by Bullock et al. (2001) (a $1\sigma \Delta(\log c_{\text{vir}}) \sim 0.18$) gives a negligible contribution to the overall error budget for the cluster masses.

The measured gravitational lensing signal is sensitive to the two-dimensional surface mass distribution, including mass associated with the cluster outside r_{500c} , and random structures seen in projection along the line of sight (Metzler, White & Loken 2001; Hoekstra 2001; Clowe, De Lucia & King 2004; de Putter & White 2005). This will introduce additional uncertainty (and potentially a net bias) to any lensing-based estimates of the cluster mass contained within a 3D volume. Studies based on simulated clusters (e.g., Clowe et al. 2004) indicate that the net bias is no more than a few percent when 3D cluster masses are estimated by fitting observations of $g_T(r)$ to predictions from theoretical models of the mass distribution, such as the NFW model. However, the scatter in the mass estimates from projection effects amount to a weak lensing mass dispersion of $\sim 15 - 25\%$ for massive galaxy clusters, which should be added to the observational uncertainties of the lensing mass estimates. In this paper, we have assumed a lensing mass dispersion of 0.26 resulting from projection effects, corresponding to the value estimated by Metzler, White & Loken (2001) from their N-body simulations. Although these authors considered a somewhat different mass estimator, more recent estimates indicate a similar mass dispersion for the NFW profile fitting method that we have used.

The absence of reliable information about the individual redshifts of the faint galaxies used for the weak lensing measurement will inevitably result in some degree of confusion between lensed background galaxies and unlensed cluster galaxies. The magnitude of this effect will depend on the projected number density of cluster galaxies, and should thus

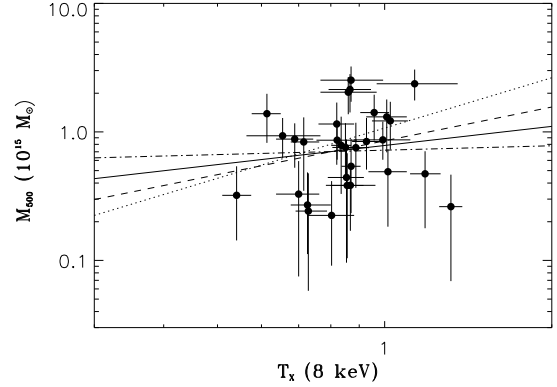


Fig. 1.— Cluster galaxy contamination in the faint galaxy catalogs as a function of distance from the cluster center. The solid line represents an average of 6 clusters at an average redshift $\bar{z} = 0.31$, while the dashed line represents an average of 5 clusters at $\bar{z} = 0.23$.

have a strong dependency on cluster radius. Hence, a radially dependent correction factor was applied to the shear measurements to correct for contamination from cluster galaxies in the faint galaxy catalogs that were used to measure the gravitational shear (these catalogs included all galaxies in the cluster fields that were detected at a signal-to-noise ratio $6 < S/N < 100$, with no additional selection based on e.g., galaxy color). The magnitude of this correction was estimated from the radial dependence of the average faint galaxy density in two “stacks” of clusters observed with the UH8K camera, one at $z \sim 0.3$ and the other at $z \sim 0.2$, assuming that the contamination is negligible at the edge of the UH8K fields, $> 1.5h^{-1}$ Mpc from the cluster center. The estimated degree of contamination is shown in Figure 1.

Eight of the clusters in our sample were also included in the combined strong and weak gravitational lensing study of S05, based on observations of a sample of 10 X-ray luminous galaxy clusters at $z \sim 0.2$ using the *Hubble Space Telescope*. These authors estimated the projected cluster mass within a clustercentric radius of $250h^{-1}$ kpc, assuming an Einstein-de Sitter ($\Omega_m = 1$, $\Omega_\Lambda = 0$) cosmology. Figure 2 shows a comparison of the mass values listed by S05 with our cluster mass estimates, using the best-fit NFW model to derive projected cluster masses, assuming the same cosmology as S05. These authors assumed a spatially constant contamination of 20% cluster galaxies in their background galaxy catalogs at radii $< 2'$, while we find an average contamination of 30% for our data at these radii. Hence, for the plot in Figure 2 we have adjusted our radially dependent contamination correction such that the average contamination at small radii is consistent with that assumed by S05. We find that our cluster mass estimates are generally consistent with those of S05, although with a tendency for slightly higher masses.

2.2. X-ray data

For clusters in the weak lensing data set, we compiled a list of corresponding X-ray temperatures from the literature. For many of these clusters, their global temperature, or even a temperature map, has been determined using data from *Chandra* and/or XMM-Newton. However, these temperatures constitute a rather heterogeneous sample, for which the systematics are not well established. Consequently, X-ray temperatures were primarily drawn from the samples of Ota & Mit-suda (2004), Allen (2000) and White (2000), each providing a

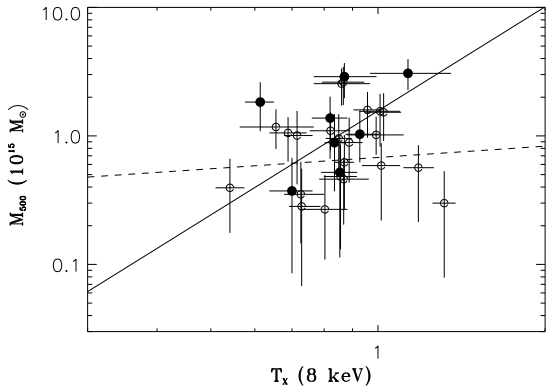


FIG. 2.— Comparison with estimates of the projected mass within $250h^{-1}$ Mpc published by S05. The lensing masses in this plot are given for the cosmological model assumed by S05. For this plot, our estimate of the degree of galaxy cluster contamination was also adjusted to match the contamination assumed by S05 (see text for details). The inner error bars represent the uncertainties associated with lensing measurements only. The outer error bars include an extra uncertainty of 26% added in quadrature to the lensing measurement uncertainty, representing the estimated spread in lensing mass estimates resulting from viewing the same cluster at different angles.

homogeneous measure of the global cluster temperature (i.e., temperature measured within a cluster-centric distance close to r_{500c}) for a major fraction of the clusters in the weak lensing sample. All these authors derived temperatures based on analysis of ASCA spectra. For two clusters not in either of the samples mentioned above we extracted published temperatures from other sources.

Specifically, from the works of Ota & Mitsuda (2004) and Allen (2000) we extracted temperatures estimated by these authors by fitting an isothermal plasma model with the Galactic absorbing column density as a free parameter to ASCA spectra. The temperatures taken from White (2000) were derived by fitting an isothermal plasma model with the nominal Galactic absorbing column density fixed, but since only energies above 1 keV are used in the White (2000) spectral fitting the fixed column density should not introduce systematic effects relative to the temperatures from the Ota & Mitsuda (2004) and the Allen (2000) samples. For the remaining two clusters we extracted published temperatures obtained in a similar way (see Table 1).

For the clusters in two or more samples, their derived temperatures agree within the uncertainties, and for any cluster the derived temperatures differ by less than 20% between samples. Also, the mean of temperature differences between any two of the samples by Ota & Mitsuda (2004), Allen (2000), and White (2000) is less than 3%, indicating the low level of systematic temperature variance between different analyses.

Although the isothermal plasma model has proven too simplistic for nearby clusters, the global cluster temperature is straightforward to derive from observations as well as simulations, enabling a rather direct comparison between observations and theory. Furthermore, for the majority of distant ($z \gtrsim 0.5$) clusters only global isothermal temperatures can be obtained in the foreseeable future. Hence, we refrain from going into the detailed spatial and spectral modeling of the intra-cluster gas. The effects of cluster dynamics, “cooling cores”, non-sphericity etc. generally affects the global temperatures only at the 10%-20% level (e.g., Evrard, Metzler, & Navarro 1996; White 2000; Smith et al. 2005).

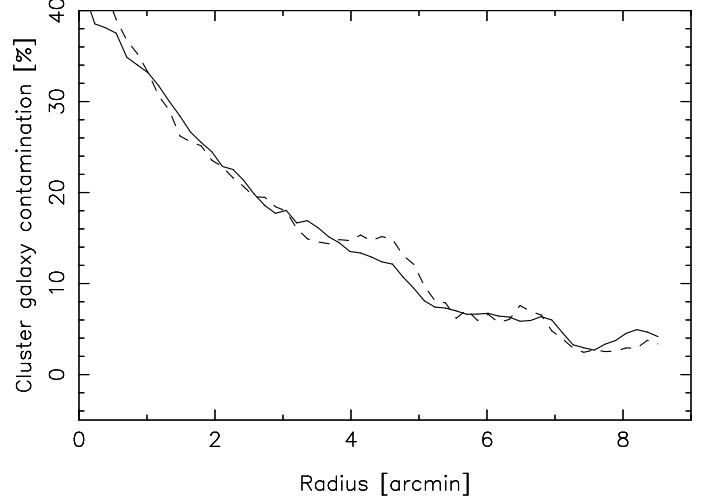


FIG. 3.— Weak lensing mass estimates and X-ray temperatures with BCES($X_2|X_1$) regression lines for different subsamples. The full line is the fit to the full sample, defined as described in the text; the dotted line is fit to Ota & Mitsuda (2004) sample; the dashed line is the fit to the Allen (2000) sample; and the dot-dashed line is the fit to the White (2000) sample.

3. RESULTS

The mass–temperature relation expected from simple theoretical arguments for a self-similar cluster population with sub-dominant non-gravitational forces is

$$\left[\frac{M_{vir}(T, z)}{10^{15}h^{-1}M_\odot} \right] = \left(\frac{T}{T_\star} \right)^{3/2} \left(\Delta_c E^2 \right)^{-1/2} \left[1 - 2 \frac{\Omega_\Lambda(z)}{\Delta_c} \right]^{-3/2}, \quad (3)$$

where Δ_c is the mean overdensity inside the virial radius in units of the critical density at the relevant redshift and $E^2 = \Omega_m(1+z)^3 + \Omega_\Lambda + \Omega_k(1+z)^2$. Using the fitting formula of Pierpaoli et al. (2001), we find that the value of Δ_c ranges from 113 (at the low-redshift end of our sample) to 124 for the clusters listed in Table 1. The redshift-dependent quantities contained in eq.3 must be calculated individually for each cluster, as they would otherwise produce an artificial 10% variation in T_\star over the redshift range spanned by our cluster sample.

We obtained mass–temperature relations by fitting the data in Table 1 using the BCES($X_2|X_1$) estimator of Akritas & Bershady (1996) to the following parameterization of the mass–temperature relation,

$$\log \left(\frac{M_{500c}}{A \times 10^{15}h^{-1}M_\odot} \right) = \alpha \log \left(\frac{kT}{8\text{keV}} \right) + \log M_0, \quad (4)$$

where A equals the product of the last two terms in eq.3, and the slope is left as a free parameter, rather than being fixed at the theoretically expected value $\alpha = 3/2$. The procedure of Akritas & Bershady (1996) takes uncertainties in temperatures as well as in weak lensing masses into account, and makes no assumptions about the intrinsic scatter of both quantities. Results from fitting sub-samples as well as the full sample are presented in Table 2 and Figure 3.

For the full data set (for those clusters with temperature from more than one sample the temperature was taken in prioritized order from Ota & Mitsuda (2004), Allen (2000), and White (2000)) we find the following normalization of the mass–temperature relation at 8 keV, at the mean redshift of our cluster sample:

TABLE 1
WEAK LENSING MASSES AND X-RAY TEMPERATURES

Cluster	z_{cl}^{a}	M_{500c} ($10^{14} h^{-1} M_{\odot}$)	kT (Ota & Mitsuda) (keV)	kT (Allen) (keV)	kT (White) (keV)	kT (other) ^b (keV)
A68	0.255	$21.37^{+6.79}_{-7.20}$	$6.93^{+0.63}_{-0.59}$
A115	0.197	$2.42^{+2.34}_{-1.84}$	$5.83^{+0.47}_{-0.30}$
A209	0.206	$7.54^{+4.24}_{-3.87}$	$7.10^{+0.40}_{-0.40}$
A267	0.230	$8.79^{+2.77}_{-3.53}$	$5.51^{+0.44}_{-0.41}$
A520	0.203	$8.67^{+3.26}_{-2.60}$...	$7.94^{+0.96}_{-0.90}$
A586	0.171	$25.27^{+7.01}_{-8.11}$	$6.96^{+0.99}_{-0.83}$	$7.02^{+0.94}_{-0.80}$	$6.06^{+0.64}_{-0.52}$...
A611	0.288	$3.83^{+2.99}_{-2.79}$	$6.85^{+0.38}_{-0.46}$...
A665	0.182	$5.40^{+3.40}_{-3.07}$	$6.96^{+0.28}_{-0.27}$	$8.12^{+0.62}_{-0.54}$	$7.73^{+0.41}_{-0.35}$...
A697	0.282	$12.18^{+4.97}_{-4.89}$	$8.19^{+0.62}_{-0.60}$...	$8.60^{+0.50}_{-0.49}$...
A773	0.217	$13.09^{+4.79}_{-6.15}$	$8.07^{+0.70}_{-0.66}$	$8.29^{+0.73}_{-0.64}$	$8.63^{+0.68}_{-0.67}$...
A959	0.285	$9.33^{+3.50}_{-3.05}$	$5.24^{+0.89}_{-0.73}$
A963	0.206	$4.42^{+4.27}_{-3.46}$	$6.83^{+0.51}_{-0.51}$	$6.13^{+0.45}_{-0.30}$	$6.08^{+0.43}_{-0.33}$...
A1576	0.299	$8.62^{+3.40}_{-2.54}$	$6.57^{+0.56}_{-0.54}$...
A1682	0.226	$2.24^{+1.51}_{-1.33}$	$6.42^{+0.63}_{-0.60}$...	$7.24^{+0.68}_{-0.59}$...
A1722	0.325	$2.70^{+2.14}_{-1.58}$	$5.81^{+0.59}_{-0.59}$
A1758N	0.280	$20.37^{+6.77}_{-6.77}$	$6.88^{+0.86}_{-0.86}$
A1763	0.228	$4.90^{+3.65}_{-3.97}$	$8.11^{+0.66}_{-0.63}$...	$7.30^{+0.46}_{-0.46}$...
A1835	0.253	$8.42^{+3.41}_{-3.33}$	$7.42^{+0.61}_{-0.43}$	$7.33^{+0.35}_{-0.30}$	$7.88^{+0.38}_{-0.46}$...
A1914	0.171	$2.62^{+2.03}_{-1.93}$	$10.53^{+0.51}_{-0.50}$...
A1995	0.320	$23.69^{+6.88}_{-6.13}$	$9.06^{+1.77}_{-1.32}$...	$7.57^{+1.07}_{-0.76}$...
A2104	0.153	$14.14^{+5.34}_{-5.55}$	$7.66^{+0.49}_{-0.43}$...	$9.12^{+0.48}_{-0.46}$...
A2111	0.229	$3.84^{+1.80}_{-2.14}$	$6.94^{+0.76}_{-0.67}$
A2204	0.152	$7.86^{+5.28}_{-4.57}$	$6.68^{+0.28}_{-0.27}$	$6.23^{+0.30}_{-0.28}$	$6.99^{+0.24}_{-0.23}$...
A2219	0.228	$4.72^{+2.35}_{-2.94}$...	$9.46^{+0.63}_{-0.57}$	$9.52^{+0.55}_{-0.40}$...
A2261	0.224	$11.52^{+5.40}_{-5.97}$	$6.56^{+0.49}_{-0.48}$	$6.64^{+0.51}_{-0.46}$	$7.49^{+0.57}_{-0.43}$...
MS1455+22	0.258	$3.21^{+2.19}_{-1.78}$...	$4.33^{+0.27}_{-0.25}$	$4.83^{+0.22}_{-0.21}$...
RX J1532.9+3021	0.345	$13.86^{+5.93}_{-5.64}$	$4.91^{+0.29}_{-0.30}$
RX J1720.1+2638	0.164	$3.28^{+2.05}_{-2.53}$	$5.60^{+0.50}_{-0.50}$
RX J2129.6+0005	0.235	$8.35^{+4.87}_{-4.82}$	$5.72^{+0.38}_{-0.30}$
Zw3146	0.291	$7.57^{+4.13}_{-3.25}$...	$6.80^{+0.38}_{-0.36}$	$5.89^{+0.30}_{-0.22}$...

^a— See Ebeling et al. (1996; 1998) for references to redshift measurements.

^b— kT value for A209 from P.B. Marty (private communication); kT value for RX J1720.1+2638 from Mazzotta et al. (2001).

$$M_{500c} = M_{8\text{keV}}(z) \times 10^{15} h^{-1} M_{\odot} \left(\frac{kT}{8 \text{ keV}} \right)^{\alpha}, \quad (5)$$

with $\alpha = 0.49 \pm 0.80$ and $M_{8\text{keV}}(z = 0.23) = M_0 A(z = 0.23) = 0.78 \pm 0.14$. It is evident that the slope of the mass-temperature relation is not well-determined since our data only span a modest range at the high mass/high temperature end of the cluster distribution. In fact, it is not obvious that there is a tight mass-temperature relation at the high temperature end probed here.

3.1. Normalization of the mass-temperature relation and σ_8

The concentration of clusters around ~ 8 keV enables a robust measurement of the normalization of the mass-temperature relation at the high-mass end. Even though the slope of the mass-temperature relation varies substantially between the three sub-samples the normalizations agree within their statistical uncertainty. We note that for all fits, the four different regressions of Akritas & Bershady (1996) all result in normalizations within 20%.

In order to obtain the strongest constraints on the mass-temperature relation normalization we take advantage of previous studies of massive clusters (Finoguenov, Reiprich, & Böhringer 2001; Allen, Schmidt, & Fabian 2001; Ar-

naud, Pointecouteau, & Pratt 2005), showing that the mass-temperature relation slope is close to $\alpha = 3/2$ as expected from simple gravitational collapse models (Kaiser 1986).

If we assume $\alpha = 3/2$ with a representative uncertainty of 10% (e.g. Finoguenov, Reiprich, & Böhringer 2001), and take $M_{\text{vir}} = 1.65 M_{500c}$ (which is the appropriate relation at the average cluster redshift for our chosen NFW model), we find $T_{\star} = 1.28 \pm 0.20$ for the full sample. Results for similar calculations of T_{\star} based on various subsamples are listed in Table 3. From the $\sigma_8 - T_{\star}$ relation plotted by Pierpaoli, Borgani, Scott, & White (2003) in their Figure 2, we find $\sigma_8 = 0.88 \pm 0.09$, based on our full sample. We note that this relation is valid only for an intrinsic scatter in temperature of $\lesssim 10\%$ around the mean mass-temperature relation. A larger intrinsic scatter will imply a lower value of σ_8 . We provide our constraints on the intrinsic scatter below.

3.2. Scatter in the mass-temperature relation

The squared scatter in lensing mass, M_{500c} , around the best fit is the sum of the squared measurement error and the squared intrinsic scatter $(\sigma_M^{\text{tot}})^2 = (\sigma_M^{\text{err}})^2 + (\sigma_M^i)^2$, and we find $\sigma_M^{\text{tot}} = 0.94$. This is larger than the mean lensing mass error, $\sigma_M^{\text{err}} = 0.52$, indicating either a sizable intrinsic scatter in

mass or that the measurement errors are under-estimated.

Accounting for errors in both mass and temperature, we find an intrinsic scatter in T_\star of $0.3^{+0.20}_{-0.30}$. There is a 77% probability that the scatter in temperature is larger than 10%, favoring somewhat lower values of σ_8 than quoted above. However, most of the scatter is caused by the low mass clusters.

3.3. Relaxed vs. non-relaxed clusters

We looked into whether relaxed clusters and non-relaxed clusters have the same normalization of the mass-temperature relation. Our “relaxed” cluster sample consists of A586, A963, A1835, A1995, A2204, A2261, RXJ1720, and RXJ1532. These are clusters with “spherical” optical and X-ray morphology, and no known cluster-scale dynamic disturbances. For the relaxed clusters we find a normalization of the mass-temperature relation of $M_{8\text{keV,relax}} = 1.56 \pm 0.32$ while the normalization for the non-relaxed clusters is $M_{8\text{keV,nonrelax}} = 0.68 \pm 0.12$ (see Figure 4). The higher normalization of relaxed clusters is supported by the fact that the mean mass of relaxed clusters is a factor 1.5 larger than the mean mass of “non-relaxed” clusters, although the relaxed and the non-relaxed clusters span roughly the same temperature range.

The scatter in mass for the relaxed sample ($\sigma_M^{\text{tot}} = 0.77$) is similar to the scatter for the non-relaxed sample ($\sigma_M^{\text{tot}} = 0.88$). The mean error for both samples is $\sigma_M^{\text{err}} = 0.57$. Either relaxed clusters spread as much around their mass-temperature relation as clusters in general, or we have used a poor definition of “relaxed” clusters. However, the fact that the normalization of the mass-temperature relation for relaxed clusters is significantly higher than for non-relaxed clusters indicates that there is a physical difference between the two sub-samples. From the present study, it thus seems that relaxed clusters do not form a tighter mass-temperature relation than clusters in general.

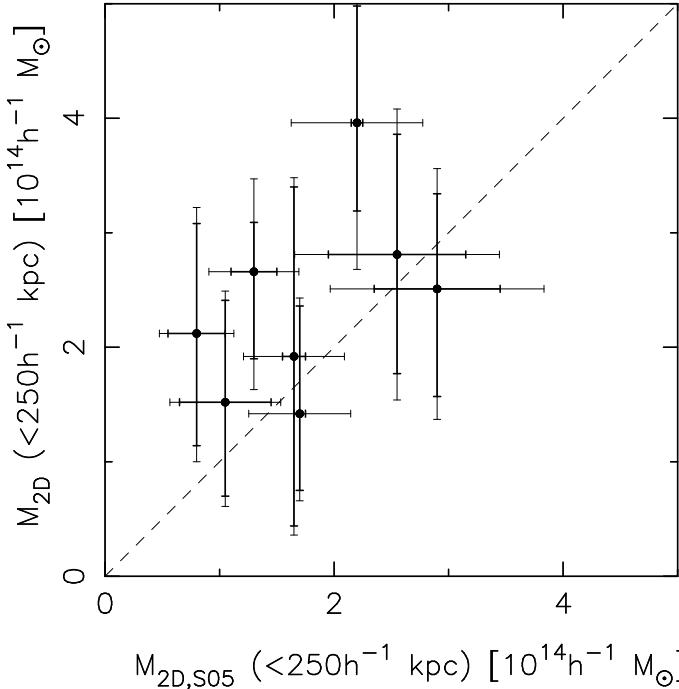


FIG. 4.— Weak lensing mass estimates and X-ray temperatures with BCES($X_2|X_1$) regressions for “relaxed” clusters (filled symbols, full line) and “non-relaxed” clusters (open symbols, dashed line).

For a given mass, non-relaxed clusters are found to be

TABLE 2
BEST-FIT MASS-TEMPERATURE RELATION (ARBITRARY SLOPE)

$M_{8\text{keV}}$	α	Sample
1.07 ± 0.22	1.30 ± 0.97	Ota & Mitsuda (2004)
0.85 ± 0.18	0.87 ± 0.78	Allen (2000)
0.72 ± 0.13	0.11 ± 0.98	White (2000)
0.78 ± 0.14	0.49 ± 0.80	All
1.56 ± 0.32	2.69 ± 1.30	“Relaxed”
0.68 ± 0.12	0.29 ± 0.76	“Non-relaxed”

TABLE 3
BEST-FIT MASS-TEMPERATURE RELATION (FIXED SLOPE)

T_\star	α	Sample
1.04 ± 0.18	$3/2$	Ota & Mitsuda (2004)
1.22 ± 0.21	$3/2$	Allen (2000)
1.35 ± 0.21	$3/2$	White (2000)
1.28 ± 0.20	$3/2$	All
0.82 ± 0.14	$3/2$	“Relaxed”
1.42 ± 0.22	$3/2$	“Non-relaxed”

NOTE. — For $\alpha = 3/2$, the uncertainty in T_\star from α has been taken to be 10%.

$\sim 75 \pm 40\%$ hotter than relaxed clusters. Since we consider global, isothermal temperatures, the presence of “cooling cores” in relaxed clusters will result in a lower global temperature than the virial temperature. However, this effect is at the 10%-20% level (e.g., Smith et al. 2003a) so this cannot alone explain the temperature difference between relaxed and non-relaxed clusters. Based on the mass-temperature relation from 10 clusters (3 of which are considered relaxed), S05 also find that non-relaxed clusters are hotter than relaxed clusters. An objective classification of the degree of relaxation for a sizeable cluster sample is required for further quantifying the size of this effect.

4. DISCUSSION

Based on the hitherto largest sample of X-ray luminous clusters with derived lensing masses, we present a normalization of the mass-temperature relation at the high mass end, $M_{8\text{keV}} = (0.78 \pm 0.14) h^{-1} 10^{15} M_\odot$. This value is higher than the lensing based mass-temperature normalization of S05, based on a smaller cluster sample, but is consistent with this within 1σ errors; see Table 4. Mass-temperature relations with masses determined from X-ray data tend to have a lower normalization than lensing based relations, and they are only marginally consistent with our normalization. This is also the case for the two recent studies of Vikhlinin et al. (2005) and Arnaud, Pointecouteau, & Pratt (2005) based on smaller samples of lower mass (and hence cooler) clusters. Vikhlinin et al. (2005) measured cluster masses inside r_{500} from X-ray observations of a sample of 13 low redshift clusters with a median temperature of 5.0 keV while Arnaud, Pointecouteau, & Pratt (2005) determined the normalization from X-ray derived masses of 10 nearby clusters with a mean temperature of 4.8 keV. The two studies agree on the same normalization, higher than previous X-ray mass based studies, but there still seems to be a $\approx 20\%$ discrepancy between X-ray and lensing derived mass-temperature relations.

TABLE 4
NORMALIZATIONS OF THE MASS-TEMPERATURE RELATION

Method	$\langle z \rangle$	$M_{8\text{keV}}(z = 0.23)$	Slope	Reference
X-rays	0.09	0.54 ± 0.04	Fitted	Arnaud, Pointecouteau, & Pratt (2005)
	0.09	0.56 ± 0.04	Fitted	Vikhlinin et al. (2005)
Lensing	0.23	0.60 ± 0.06	Fixed	S05
	0.23	0.78 ± 0.14	Fitted	This study
Simulations	0.04	0.68 ± 0.10	Fixed	Evrad, Metzler, & Navarro (1996)
	0.00	0.57 ± 0.06	Fitted	Borgani et al. (2004)

NOTE. — Included here are some recent studies with a quoted normalization of the $M_{500} - T$ -relation, scaled to $M_{8\text{keV}}$, i.e., the mass contained within r_{500} of a cluster with $kT = 8\text{keV}$, with errors propagated, and assuming $h = 1$. The listed normalization has been scaled to a common redshift of $z = 0.23$, assuming the redshift dependence expected for a self-similar collapse model, as given by eq. 3. The normalization of S05, which was determined within a fixed physical radius of $250h^{-1}$ kpc in an Einstein-de Sitter universe, has been scaled to M_{500} for our adopted cosmology, making the same assumptions about an NFW-type mass profile as we have made for our own data. For each study, we indicate whether the slope of the relation was calculated from a fit to the data, or whether the slope was fixed at the theoretically expected value.

We note, however, that the lensing based and X-ray based normalizations are made at different redshifts, and that this discrepancy would vanish if the redshift-dependence predicted by the self-similar collapse model in equation 3 were neglected. Given the heterogeneous nature of these data sets, any claim of significant departures from self-similarity would be premature, but this clearly provides an interesting avenue for future research, involving even larger cluster samples spanning a wider interval in redshift.

We confirm the result of Smith et al. (2005) that non-relaxed clusters are on average significantly hotter than relaxed clusters. This is qualitatively consistent with N-body/hydrodynamical cluster simulations which show that major mergers can temporarily boost the X-ray luminosities and temperatures well above their equilibrium values (e.g. Randall et al. 2002).

In contrast to several previous (mainly X-ray mass based) published mass-temperature relations, the normalization derived in this study is in good agreement with the normalization derived from numerical simulations. However, the accuracy of the normalization is not good enough to discriminate between simulations including different physical processes.

Our results show that X-ray based measurements of the cluster abundances, after reducing the major systematic uncertainties associated with the mass-temperature normalization, give an amplitude of mass fluctuations on cluster scales that is consistent with other methods. This lends additional support to the “concordance model” cosmology, and lends credence to the basic assumptions of Gaussian density fluctuations. Our determination of $\sigma_8 = 0.88 \pm 0.09$ is higher than most of the recent σ_8 determinations from cluster data (for a compilation of these, see e.g., Henry 2004). However, our finding is consistent with the value derived from weak gravitational lensing in the combined Deep and Wide CFHT Legacy Survey ($\sigma_8 = 0.86 \pm 0.05$; Sembolini et al. 2005) based on the halo model of density fluctuations (Smith et al. 2003b). It is also consistent with the CMB+2dFGRS+Ly α forest result ($\sigma_8 = 0.84 \pm 0.04$) of Spergel et al. (2003), with the joint CMB + weak lensing analysis of Contaldi, Hoekstra, & Lewis (2003), which gave $\sigma_8 = 0.89 \pm 0.05$, and with recent CMB analyses (Bond et al. 2005) yielding $\sigma_8 \approx 0.9$. Hence, there is now good agreement between a wide variety of meth-

ods to determine σ_8 . We caution, however, that our quoted value of σ_8 is based on the assumption that the intrinsic scatter about the mass-temperature relation is $\lesssim 10\%$, and that our σ_8 estimate will be biased high if the true scatter significantly exceeds this value (Pierpaoli, Borgani, Scott, & White 2003).

The limiting factor of our measurement of the normalization of the mass-temperature relation is the magnitude of the measurement errors. In order for the mass-temperature relation to be a competitive route for constraining cosmological parameters and to discriminate between simulations with different input physics, the normalization must be measured to better than $\sim 10\%$ accuracy. However, there are good prospects for improving on these results in the near future. Firstly, the superior spectro-imaging capabilities of *Chandra* and XMM-Newton will allow the construction of large, homogeneous cluster temperature samples. A comparison to tailored simulations with realistic physics, analyzed in the same way as observations, will advance our understanding of systematics and the link between the mass-temperature relation and structure formation (C.B. Hedenfeld et al. 2006, in preparation). Secondly, more accurate weak lensing-based mass measurements of a larger sample of clusters are feasible as large mosaic CCD cameras that can probe intermediate-redshift clusters beyond their virial radii are now common, and the cluster sample could easily be doubled from a similar survey in the Southern celestial hemisphere.

Finally, we note that a more direct measurement of σ_8 from weak lensing by clusters is feasible, provided that weak lensing mass estimates are available for a large, well-defined, volume-limited cluster sample. This makes it feasible to calculate the cluster mass function directly from the lensing masses, rather than indirectly via the X-ray temperature function (Dahle 2006). Since mass estimates based on baryonic tracers of the total cluster mass only enters indirectly as a selection criterion (e.g., clusters selected based on X-ray luminosity above a certain threshold), the method will be less susceptible to systematic and random errors, as it does not require an accurate characterization of the scatter around the mean mass-temperature relation.

We thank Per B. Lilje and Jens Hjorth for valuable com-

ments on a draft version of this paper. KP acknowledges support from the Danish National Research Council, the Carlsberg foundation, and Instrument Center for Danish Astrophysics. The Dark Cosmology Centre is funded by the Dan-

ish National Research Foundation. HD acknowledges support from the Research Council of Norway and travel support from NORDITA.

REFERENCES

Akritas, M. G. & Bershady, M. A. 1996, *ApJ*, 470, 706
 Allen, S. W. 2000, *MNRAS*, 315, 269
 Allen, S. W., Schmidt, R. W., & Fabian, A. C. 2001, *MNRAS*, 328, L37
 Arnaud, M., Pointecouteau, E., & Pratt, G. W. 2005, *A&A*, 441, 893
 Bond, J.R., et al. 2005, *ApJ*, 626, 12
 Borgani, S., Girardi, M., Carlberg, R. G., Yee, H. K. C., & Ellingson, E. 1999, *ApJ*, 527, 561
 Borgani, S., et al. 2004, *MNRAS*, 348, 1078
 Böhringer, H. et al. 2003, *ApJ*, 566, 93
 Briel, U. G. & Henry, J. P. 1993, *A&A*, 278, 379
 Bullock, J. S., Kolatt, T. S., Sigad, Y., Somerville, R. S., Kravtsov, A. V., Klypin, A. A., Primack, J. R., & Dekel, A. 2001, *MNRAS*, 321, 559
 Carlberg, R. G., Morris, S. L., Yee, H. K. C., & Ellingson, E. 1997, *ApJ*, 479, L19
 Contaldi, C. R., Hoekstra, H., & Lewis, A. 2003, *Physical Review Letters*, 90, 221303
 Clowe, D., De Lucia, G., & King, L. 2004, *MNRAS*, 350, 1038
 Dahle, H., Kaiser, N., Irgens, R. J., Lilje, P. B., & Maddox, S. J. 2002, *ApJS*, 139, 313
 Dahle, H. 2006, *ApJ*, to be submitted
 de Putter, R., & White, M. 2005, *New Astronomy*, 10, 676
 Ebeling, H., Voges, W., Böhringer, H., Edge, A. C., Huchra, J. P., & Briel, U. G. 1996, *MNRAS*, 281, 799
 Ebeling, H., Edge, A. C., Böhringer, H., Allen, S. W., Crawford, C. S., Fabian, A. C., Voges, W., & Huchra, J. P. 1998, *MNRAS*, 301, 881
 Ebeling, H., Edge, A. C., Allen, S. W., Crawford, C. S., Fabian, A. C., & Huchra, J. P. 2000, *MNRAS*, 318, 333
 Eke, V. R., Navarro, J. F., & Frenk, C. S. 1998, *ApJ*, 503, 569
 Evrard, A. E., Metzler, C. A., & Navarro, J. F. 1996, *ApJ*, 469, 494
 Finoguenov, A., Reiprich, T. H., & Böhringer, H. 2001, *A&A*, 368, 749
 Frenk, C. S., White, S. D. M., Efstathiou, G., & Davis, M. 1990, *ApJ*, 351, 10
 Henry, J. P. 2004, *ApJ*, 609, 603
 Heymans, C., et al. 2005, *ArXiv Astrophysics e-prints*, arXiv:astro-ph/0506112
 Hjorth, J., Oukbir, J., & van Kampen, E. 1998, *MNRAS*, 298, L1
 Hoekstra, H. 2001, *A&A*, 370, 743
 Huterer, D. & White, M. 2002, *ApJ*, 578, L95
 Kaiser, N. 1986, *MNRAS*, 222, 223
 Mazzotta, P., Markevitch, M., Vikhlinin, A., Forman, W. R., David, L. P., & VanSpeybroeck, L. 2001, *ApJ*, 555, 205
 Metzler, C. A., White, M., & Loken, C. 2001, *ApJ*, 547, 560
 Navarro, J. F., Frenk, C. S., & White, S. D. M. 1997, *ApJ*, 490, 493
 Ota, N., & Mitsuda, K. 2004, *A&A*, 428, 757
 Pen, U. 1998, *ApJ*, 498, 60
 Pierpaoli, E., Scott, D., & White, M. 2001, *MNRAS*, 325, 77
 Pierpaoli, E., Borgani, S., Scott, D., & White, M. 2003, *MNRAS*, 342, 163
 Randall, S. W., Sarazin, C. L., & Ricker, P. M. 2002, *ApJ*, 577, 579
 Reiprich, T. H. & Böhringer, H. 2002, *ApJ*, 567, 716
 Rosati, P., Borgani, S., Norman, C. 2002, *ARA&A*, 40, 539
 Sanderson, A. J. R., Ponman, T. J., Finoguenov, A., Lloyd-Davies, E. J., Markevitch, M., Reiprich, T. H. & Böhringer, H. 2002, *MNRAS*, 340, 989
 Seljak, U. 2002, *MNRAS*, 337, 769
 Semboloni, E., et al. 2005, *ArXiv Astrophysics e-prints*, arXiv:astro-ph/0511090
 Smith, G. P., Edge, A. C., Eke, V. R., Nichol, R. C., Smail, I., & Kneib, J. 2003a, *ApJ*, 590, L79
 Smith, R. E., et al. 2003b, *MNRAS*, 341, 1311
 Smith, G. P., Kneib, J.-P., Smail, I., Mazzotta, P., Ebeling, H., & Czoske, O. 2005, *MNRAS*, 359, 417
 Spergel, D. N., et al. 2003, *ApJS*, 148, 175
 Vikhlinin, A. et al. 2005, *ApJ*, 628, 655
 White, D. A. 2000, *MNRAS*, 312, 663